GL01375

VOL. 82, NO. 17 JOURNAL OF GEOPHYSICAL RESEARCH JUNE 10, 1977

DIFFERENTIAL THERMAL EXPANSION OF PORE FLUIDS: FRACTURE PROPAGATION AND MICROEARTHQUAKE PRODUCTION IN HOT PLUTON ENVIRONMENTS

Richard B. Knapp and Jerry E. Knight

Department of Geosciences, University of Arizona, Tucson, Arizona 85721

Abstract. Thermally induced differential expansion between fluid in isolated pores and enclosing minerals decreases effective pressure at the pore-mineral interface. With a sufficient increase in temperature, effective pressure becomes equal to the tensile strength, and the rock fractures. The ratio of the coefficient of thermal expansion to the compressibility for the pore fluid defines the nature of this process. Finite element computations indicate that thermally induced hydraulic fracturing of host rocks is inevitable in hot pluton environments. A fracturing front propagates away from cooling plutons at a rate of 100 cm/yr for the first 400 years and at 1 cm/yr at 10^5 years. Fluid energy release upon fracturing can produce microearthquakes of measurable magnitude. Predicted frequencies of microearthquakes vary from 4×10^3 events/day at 5×10^3 years to 500 events/day at 10^5 years. Estimates of ambient pore fluid pressures and effective pressures show that effective pressure continually increases with depth for geothermal gradients less than 10°C/km. For larger geothermal gradients the effective pressure first increases but eventually decreases.

Introduction

The generation of microcracks and larger-scale fractures has been attributed to differential compression and thermal contraction between minerals [Nur and Simmons, 1970] and to tectonic processes. In this study we quantitatively examine a process suggested by Norris and Henley [1976] whereby cracks may be produced by differential thermal expansion between fluid in isolated fluid-filled pores and encasing minerals. A temperature increase in rocks results in an increase in pore fluid pressure, which decreases the effective pressure $P_e = P_c - P_f$ at the pore-mineral boundary. Fracturing ensues when effective pressure becomes less than the tensile strength of the rocks [Hubbert and Willis, 1957; Hubbert and Rubey, 1959].

Any geologic environment characterized by increasing temperatures can potentially be a site of thermally induced hydraulic fracturing. Hot pluton environments are probably the most significant, since large quantities of thermal energy are dispersed over large volumes of rock [Norton and Knight, 1977]. Other sites of possible importance are areas of an increasing regional heat flux and burial environments in which rocks experience an increase in confining pressure as well as temperature. The role of temperature in creating anomalously large pore fluid pressures in burial environments has been qualitatively examined by Barker [1972].

We consider only isolated pores in this study. The fact that isolated pores compose approximately 90% of the total porosity in crystalline, as well as some sedimentary, rocks [Norton and Knapp, 1977] justifies this restriction. These isolated pores occur along grain boundary discontinuities, and we therefore choose a rock tensile strength of zero. Even moderate deviations from this failure criterion will not seriously affect the conclusions.

Thermally induced strains and stresses in minerals, pressures in fluid-filled pores, and the dynamic interaction between fluid and rock are computed in this study. The nature of these stresses and strains has been analyzed using equations derived for the force displacement finite element method [Zienkiewicz, 1971, pp. 16-33].

Equation Development

Fluid Elements

A combination of elastic and fluid properties in a single finite element structural system requires a constant mass fluid element consistent with the force displacement finite element method. There appears to be no derivation in the literature for such an element, though Belytschko and Kennedy [1975] have developed a constant pressure fluid element. A constant mass fluid element can be based on the total derivative of volume at constant composition:

$$dV = V_I \alpha \, dT - V_I \beta \, dP \qquad (1)$$

Additional assumptions of isothermal expansion or compression and the independence of β and dV over a single temperature increment permit (1) to be rearranged and integrated to give the incremental forces due to a change in volume:

$$\Delta \underline{F} = \Delta P \cdot \underline{A} = - \frac{\Delta V \underline{A}}{V_I \beta} \qquad (2)$$

Equation (2) may be solved by determining the change in volume of an element due to nodal displacements and then resolving the resultant change in pressure to forces at the node points. The volume change for individual elements in response to unit node point displacements is determined by a matrix obtained by differentiating the element interpolation functions [Zienkiewicz, 1971, pp. 115-120]:

Paper number 7B0029.

$$\underline{\Delta V} = \nabla \underline{T}_{u,p} \tag{3}$$

Forces at the node points are obtained by resolving the pressure on each face of the element into X and Y force components and placing half the value of each component on each of the nodes which define the face. For a two-dimensional triangle of thickness t the result is

$$\underline{T}_{f,p} = \frac{-t}{2V_I\beta}\,[(m_{31}L_{31} - m_{12}L_{12}),$$
$$(l_{12}L_{12} - l_{31}L_{31}),\ (-m_{23}L_{23} - m_{12}L_{12}),$$
$$(l_{23}L_{23} + l_{12}L_{12}),\ (m_{31}L_{31} - m_{23}L_{23}),$$
$$(l_{23}L_{23} - l_{31}L_{31})]^T \tag{4}$$

where the superscript T denotes matrix transposition.

Node point forces per unit displacement of node points are determined by the matrix obtained by multiplying (3) and (4):

$$\underline{K}_{fluid} = \underline{T}_{f,p} \cdot \underline{\Delta V} \tag{5}$$

The column sums of $\underline{K}_{fluid}$ are zero, as required by force equilibrium criteria. Furthermore, $\underline{K}_{fluid}$ is required to be asymmetric and singular and thus distinguishable from the equivalent matrix of an elastic element, which is defined as [Zienkiewicz, 1971, p. 25]

$$\underline{K}_{elastic} = \int \underline{T}^T_{e,p}\ \underline{D}\ \underline{T}_{e,p}\ dV \tag{6}$$

Thermal Stresses

The derivative of fluid pressure in a fluid element with respect to temperature is also obtained from (1), which upon a change of variables and rearrangement reduces to

$$\left(\frac{dP}{dT}\right)_V = \frac{\alpha}{\beta} \tag{7}$$

The pressure change due to a unit increase in temperature is then converted to resultant nodal forces by multiplying the finite difference form of (7) by (4).

Numerical Solutions

The isolated pore-rock system is approximated by a finite element discretization. A discretization of 64 elements and 37 nodes is used to represent a circular pore 1.5×10^{-3} cm in radius in a square section of rock 2.4×10^{-2} cm on a side and unit thickness. Due to symmetry, only one quarter of the system is considered.

Temperature derivatives of (5) and (6) are approximated by an incremental method whereby nodal coordinates, stresses, fluid pressure, temperature, and material properties are updated after each incremental temperature step. Temperature step sizes of 5°C or less are chosen so that changes in the volume of the fluid elements are $\leq$0.01%. Pore fluid is assumed to be approximated by the H_2O system [Keenan et al., 1969; Helgeson and Kirkham, 1974]. The coefficient of volumetric-isobaric thermal expansion and its temperature derivative for quartz [Skinner, 1966], and Young's modulus and Poisson's ratio, along with their temperature derivatives for silica glass [Birch, 1966], are used to represent the rock properties. All rock properties are assumed to be independent of pressure, consistent with the fact that moderate changes in the rock properties will not appreciably affect the results.

We emphasize here that as used in this study (5)-(7) are valid only until the chosen failure criterion is met. At that time they are no longer an accurate approximation.

Analysis

Pressure Coefficient of the H_2O System

The pressure coefficient α/β for the H_2O system has values between 10 bars/°C and 25 bars/°C for all ambient subsurface conditions in the upper 30 km of the earth's crust (Figure 1); a 1° increase in temperature produces at least a 10-bar increase in pore fluid pressure, provided the pore volume remains constant. This suggests that differential thermal expansion between pore fluid and enclosing minerals is a potentially important process for decreasing effective pressure in any crustal region, since only moderate increases in temperature (100°C) produce large increases in fluid pressure (>1 kbar).

Changes in pressure and temperature have a significant effect on the value of the pressure coefficient. The derivative of α/β with respect to pressure at constant temperature is positive for all temperatures and pressures considered but approaches zero at fluid pressures greater than about 5 kbar (Figure 1). For constant fluid pressures less than 2 kbar the pressure coefficient sharply increases with temperature until it reaches a maximum at about 150°C (Figure 2). The pressure coefficient α/β decreases with further increases in temperature and becomes less temperature sensitive at higher fluid pressures, but the maximum at 150°C persists throughout (Figure 2). Thus the largest rates of fluid pressure increase with respect to temperature occur between 100 and 300°C.

Pressure Variations With Depth

Pore fluid pressure and effective pressure are poorly known quantities for igneous and metamorphic rocks in the earth's crust. In this study, equilibrium pore fluid and effective pressure as a function of depth were estimated by computer experiments in which confining pressure and temperature were incrementally increased on the rock section. The increment in confining pressure, chosen to be equivalent in all directions, was equal to the product of the lithostatic gradient for a uniform rock density of 2.75 g/cm^3 and the depth increment. These pressures were converted to nodal boundary loads. The temperature increment was determined by the chosen constant geothermal gradient and the change in depth. Symmetry conditions were used to define the displacement boundary conditions. The initial condition in all cases was a rock at the surface with an initial stress and pore fluid pressure of 1 bar and an initial temperature of 10°C.

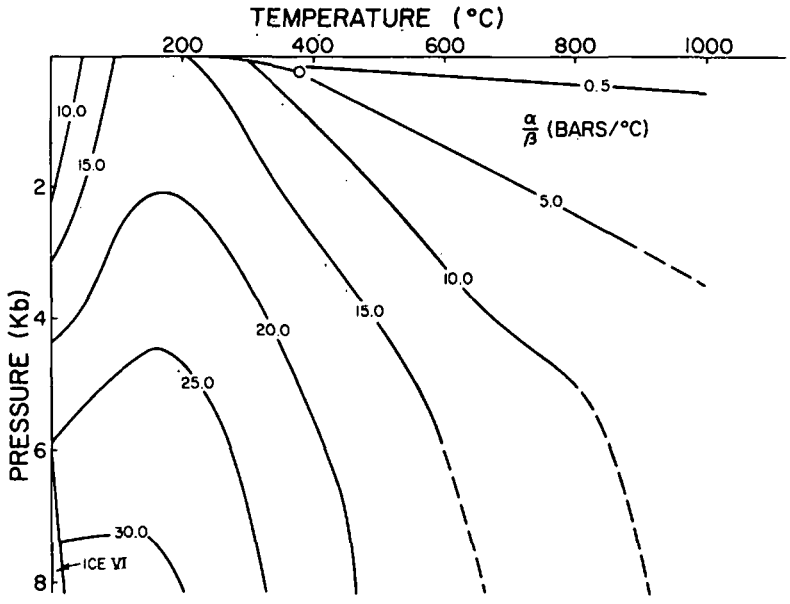

Fig. 1. Values of the pressure coefficient α/β over a wide range of temperatures and fluid pressures in the H_2O system. The open circle and attached line denote the critical endpoint and two-phase curve, respectively. Data from Keenan et al. [1969] and Helgeson and Kirkham [1974].

The results show that the value of pore fluid pressure for a given depth is dependent on the value of the geothermal gradient (Figure 3). Furthermore, pore fluid pressure increases only slightly at depths less than 5 km; at greater depths it increases at a larger rate.

The effective pressure will decrease as temperature and confining pressure increase only if

$$\frac{\alpha}{\beta} \geq \frac{dP_c}{dz}\frac{dz}{dT} \qquad (8)$$

where z is positive downward. The variation of the pressure coefficient with depth and the depth at which the critical value, defined by (8), is attained are shown for various geothermal gradients in Figure 4. This critical value is realized at 0.8 km and 2.6 km for the 30°/km and 20°/km geothermal gradient, respectively, and results in zero effective pressure at depths of 2 and 6.6 km (Figure 5). The 10°/km geothermal gradient is the largest gradient for which the critical value of α/β is never reached. At this gradient the effective pressure continually increases (Figure 5). Equation (8), however, does not insure that the effective pressure at the pore boundary will subsequently decrease to zero before α/β again drops below the critical value. The minimum geothermal gradient at which the effective pressure goes to zero is 15°/km

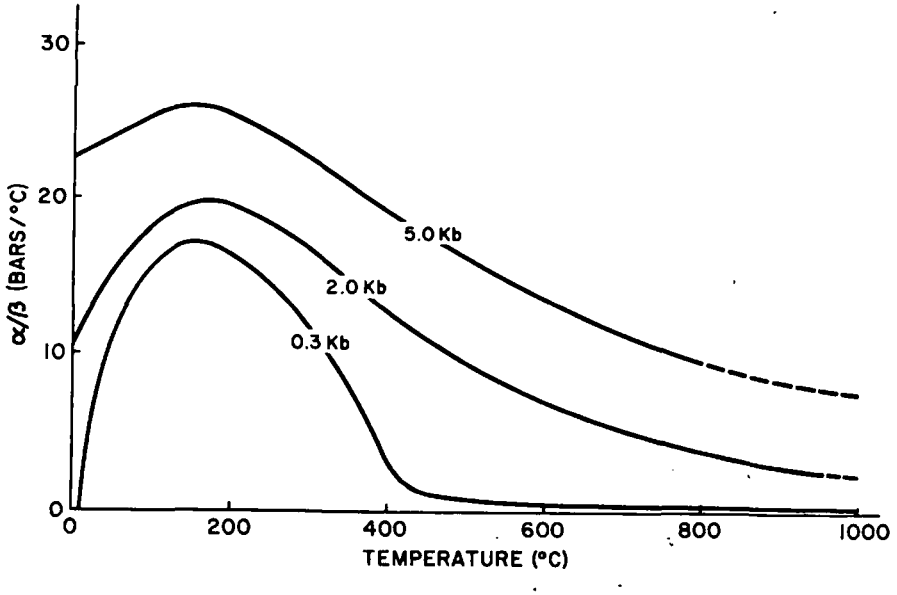

Fig. 2. Isobaric sections through Figure 1.

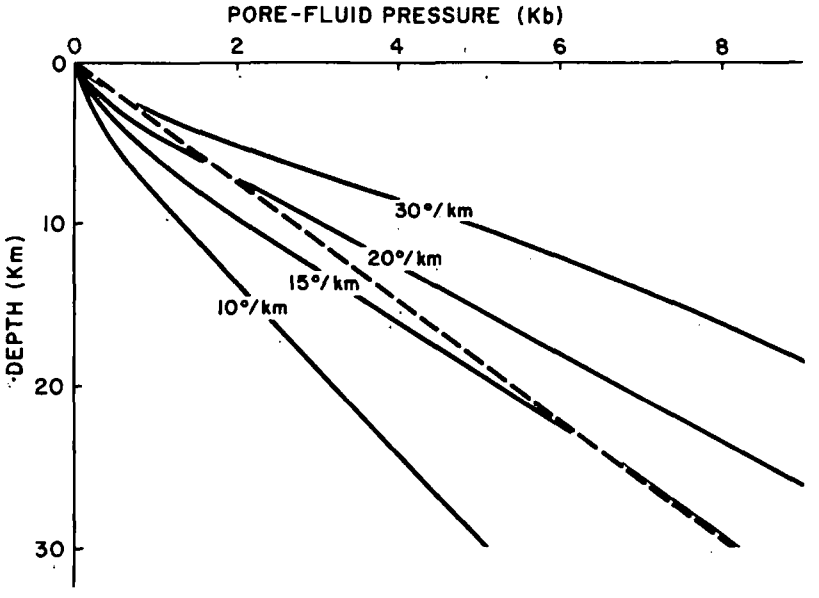

Fig. 3. Pore fluid pressure at depth for various geothermal gradients. The dashed line is the hydrostatic confining pressure calculated for a rock with a uniform density of 2.75 g/cm^3.

(Figure 5). Therefore 14°/km is the maximum gradient at which a circular pore is stable throughout the entire crust. Anomalously high pore fluid pressures initially observed in oil wells along the northern coast of the Gulf of Mexico are consistent with the above predictions, since the ambient geothermal gradient in this burial environment is inferred to be greater than 18°/km [Barker, 1972].

The significance of the predicted zero effective pressure for geothermal gradients greater than 14°/km is not entirely clear. Gradients greater than 14°/km may not persist at depth, or the effective pressure may reach zero. It is interesting to note that for the gradients most commonly taken as average, 20°/km to 15°/km, the predicted depths of zero effective pressure are within crustal zones of anomalously large electrical conductivities [Keller, 1971] and small P wave velocities [Landisman et al., 1971]. These data are consistent with the increased fracture abundance expected under conditions of zero or negative effective pressure.

Pore fluid pressure variations with depth, for the condition that the horizontal stress equals 0.8 of the lithostatic load, do not differ significantly from the values predicted for the case in which the confining pressure was equal in all directions. The only effect was a decrease in the depth at which zero effective pressures occur due to the decrease in the least compressive stress. An experiment with an elliptical pore with an aspect ratio of 1:3 was also computed. As was predicted by Walsh [1965], failure occurred at shallower depths for elliptical pores than for circular pores, due to stress concentrations at the tips of the ellipse, even though the effective pressure was greater than zero. These factors indicate that depths to zero effective pressure given in Figure 5 are maximum values.

Having estimated ambient pore fluid and effective pressures, some consequences and implications of thermally induced increases in pore fluid pressure can be examined. The hot pluton environment serves as an exemplary basis for this examination and is the environment used in this study.

Fracture Propagation

Heated host rocks in hot igneous pluton envi-

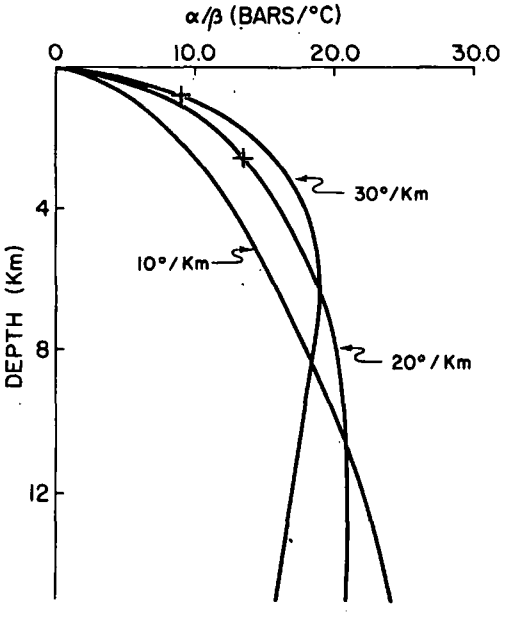

Fig. 4. Values of the pressure coefficients at depth for various geothermal gradients. The plus sign denotes the value and depth at which the critical value of the pressure coefficient (equation (8)) is reached.

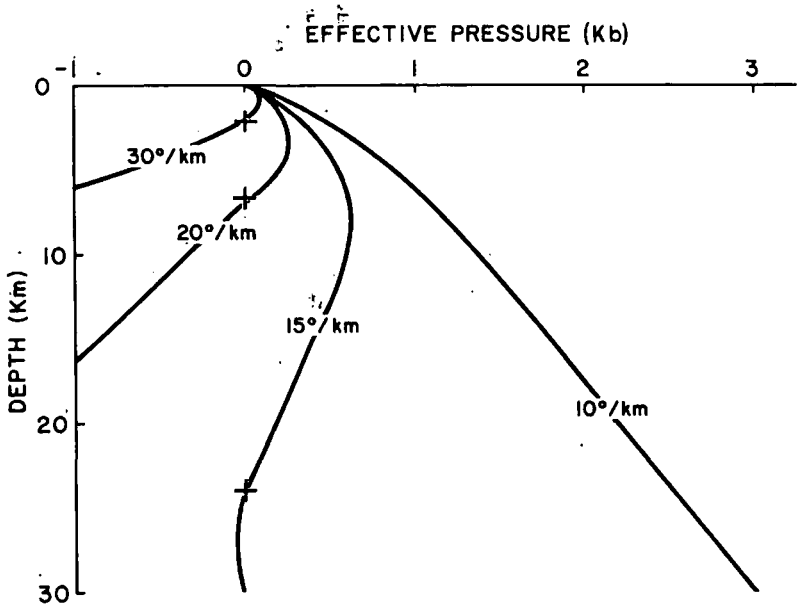

Fig. 5. Effective pressure at depth for various geotherms. Plus signs denote depths of zero effective pressure.

ronments are likely to have anomalously low effective pressures. Transport of heat from the intrusive into the host rocks clearly causes fluid pressure increases in isolated fluid-filled pores, and for sufficiently large increases the effective pressure will become zero and the rock will fracture. Changes in effective pressure with time for host rocks around a cooling pluton have been examined. The thermal history of an impermeable pluton with an initial temperature of about 850°C emplaced at a depth of 4.5 km into impermeable host rocks with a background geothermal gradient of 20°/km was used as a basis for the computations. See Norton and Knight's [1977] model P3 for more details. The pore fluid and effective pressures defined in Figures 3 and 5, respectively, were used as initial conditions in the calculations. Displacement boundary conditions were defined from symmetry considerations.

Host rocks immediately adjacent to the hot intrusive are instantaneously heated to a temperature equal to one half of the pluton's anomalous temperature [Lovering, 1935; Jaeger, 1968]. For typical magmas this amounts to an instantaneous temperature increase of about 400°C and a pore fluid pressure increase of at least 4 kbar, which results in large negative values of effective pressure and abundant fracturing. Even large deviations from the initial conditions given in Figures 3 and 5 do not alter this conclusion.

As the pluton cools and crystallizes, a zero effective pressure front propagates away from the pluton in a concentric pattern, due to the dispersal of heat into the host rocks and the subsequent temperature increase (Figure 6). The velocity of propagation of the front averages 100 cm/yr for the first 400 years after emplacement and decreases to 1 cm/yr at 10^5 years (Figure 7). It is important to note that the pluton is completely crystalline at 5×10^4 years and that the fracture front continues to propagate for significantly longer times.

Host rocks in the vicinity of hot plutons are undoubtedly fractured as a result of decreased effective pressure. Increased permeability, which undoubtedly accompanies fracturing, facilitates convective heat transfer, which increases the rate of heating of all rocks above the pluton. This, in turn, accelerates the propagation of the zero effective pressure front and fracturing. To the sides of the pluton, convective heat transfer decreases the rate of heating [Norton and Knight, 1977] and results in decelerating the outward propagation of fracturing. As such, the rates suggested in Figure 7 are minimums above the pluton and maximums to the flanks.

Pluton intrusion may be augmented by this decrease in effective pressure and instantaneous development of host rock fractures near the hot pluton-host rock boundary. Decreased effective pressure and increased fracture abundance have the effect of reducing the strength of the rock. Therefore smaller buoyancy forces are required for intrusion of a magma. Increasing fracturing

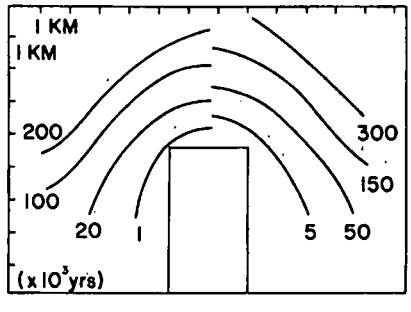

Fig. 6. Isochrons of the zero effective pressure front plotted in two-dimensional cross section of cooling pluton. Times are in thousands of years after emplacement. The pluton is cooling by pure conduction and is completely crystalline at about 50,000 years.

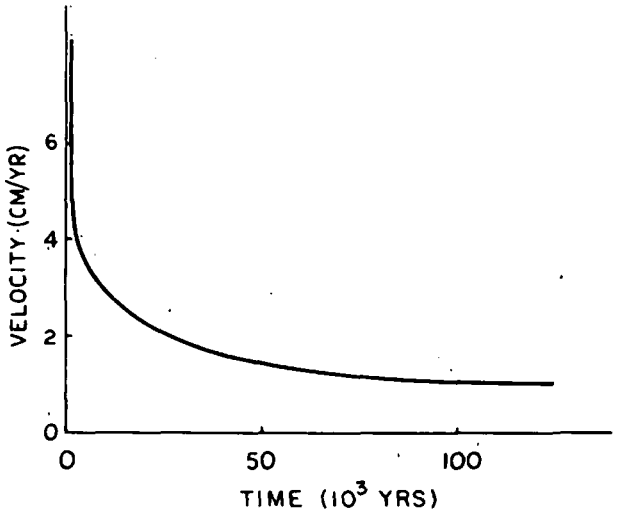

Fig. 7. Speed of propagation of the zero effective pressure front versus elapsed time for pluton environment in Figure 6.

abundance also facilitates intrusion by host rock stoping.

Microearthquake Production

Thermally induced hydraulic fracturing occurs upon reduction of the effective pressure at the pore-mineral boundary to a value equal to the rock's tensile strength, essentially zero. During fracturing, energy is released by the return of the rock to equilibrium stress conditions and by the expansion of pore fluid to an equilibrium state. A microearthquake will result if at least some of this stored energy is released in the form of seismic waves.

Elastic strain energy is stored in the rock as a result of thermal and tectonic stresses. In an isothermal fracturing event there is negligible release of elastic strain energy stored from the action of thermal stresses. For simplicity, we assume that there is no tectonically induced elastic strain energy in the system under consideration.

Therefore the total fluid energy available for release in an isothermal fracturing event is the sum of the fluid potential energies E stored within all fluid-filled pores involved in the event. For a single pore,

$$E = \int_{P_I,V_I}^{P_o,V_o} P\, dV \qquad (9)$$

where the I subscript denotes the state immediately prior to fracturing and the o subscript denotes the equilibrium state after fracturing. In this study (9) is approximated by assuming that pressure is a linear function of volume. The work done by the fluid-filled pore on the enclosing minerals is considered positive.

We examine the two end-member cases of the equilibrium state after fracturing (Figure 8). Case I represents the condition where fracturing has occurred but the pore remains isolated. The pore fluid pressure remains equal to the confining pressure, and only an infinitesimal increase in temperature is required to further propagate the fracture. The energy release in case I is negligible.

Case II (Figure 8) represents the condition where fracturing has occurred and the previously isolated pore now intersects a throughgoing fracture within which the fluid pressure equals the fluid hydrostatic pressure at that depth. The pore fluid pressure change in this case can be significant, and considerable energy can be released. The fracturing of one pore with a volume of 3.4×10^{-9} cm^3 releases 2×10^{-8}J, which from the Gutenberg-Richter equation for surface waves [Bath, 1966],

$$M = \frac{(\log E) - 4.71}{1.68} \qquad (10)$$

produces an undetectable -7.4 surface wave magnitude microearthquake. A zero magnitude earthquake can be produced if all pores in a cubic meter of rock with a total porosity of 0.01 fracture simultaneously. A 3.6 magnitude earthquake can be produced for a 10^{-3} km^3 volume of the same rock.

It is emphasized that the assumption that all pores fracture simultaneously and that energy conversion is 100% efficient is idealized. Simultaneous fracturing is augmented, however, by shock wave propagation. These calculations therefore represent maximums. We also reiterate that the quantitative prediction of pore fluid pressure variations with temperature is only valid before fracturing occurs.

The frequency of microearthquake production

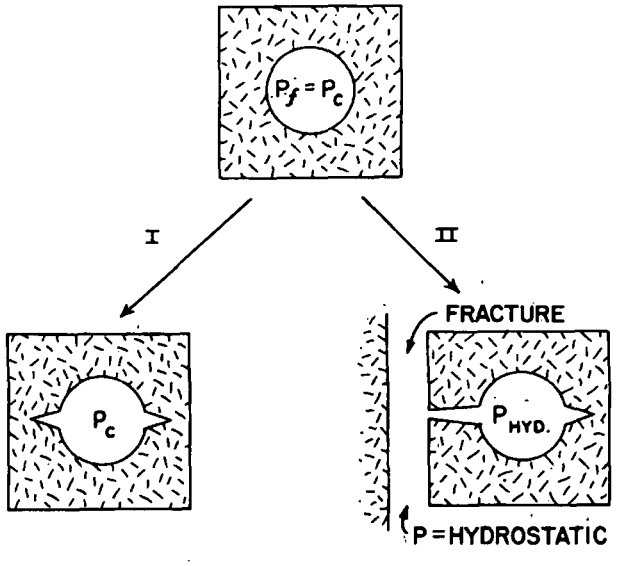

Fig. 8. Schematic of equilibrium conditions immediately prior to and after fracturing of an isolated pore. End members of possible final equilibrium states are shown (I and II). In case I the pore remains isolated and the final pore fluid pressure P_f equals the confining pressure P_c. In case II the fractured pore intersects another fracture within which the fluid pressure is hydrostatic, P_{HYD}.

in the cooling plutonic system has been predicted from the velocity of propagation of the fracturing front (Figure 7) and the energy release per unit volume of rock upon fracturing. The frequency of production for microearthquakes with a magnitude of zero varies in time from over 10^4 events/day for the first thousand years after emplacement of the pluton to about 500 events/day at an elapsed time of 10^5 years (Figure 9). Though convective heat transfer in the host rocks would change the shape of this curve, the area beneath the curve remains constant, reflecting a change in the rate and not the quantity of energy release.

Due to the inferred presence of a hot pluton at depth, microearthquake activity in present-day geothermal areas and active volcanoes serves as observational data for the proposed mechanism. Studies at the Coso geothermal area [Combs, 1975], the Dunes geothermal area [Jarzabek and Combs, 1976], the Kilbourne Hole area [Johnson and Combs, 1976], and the Radium Springs area [Quillin and Combs, 1976] indicate that microearthquake frequencies vary between about 5 and 100 events/day in known geothermal resource areas. These values are considerably lower than those predicted in Figure 9. Clearly, part of this discrepancy is due to the idealized nature of the assumptions that result in the predicted frequencies being maximums. However, the age of the geothermal system must be considered since the theory predicts lower frequencies for increasingly older systems. We therefore suggest that at least some of the microearthquakes observed in present-day geothermal systems result from thermally induced hydraulic fracturing of isolated fluid-filled pores. Furthermore, this seismic activity does not require the presence of a magma body at depth, since microearthquake production continues after the pluton is completely crystalline and cooled to nearly ambient conditions.

Microearthquake swarms in regions of active volcanism are in sharp contrast to the activity in geothermal areas. Monthly frequencies as large as 1.4×10^4 and a maximum daily frequency of 3×10^3 were recorded by Minakami et al. [1969] for the Ebino earthquake swarm. Most of the recorded microearthquakes had magnitudes slightly less than zero. These observed frequencies agree reasonably well with the frequencies predicted in this study for recently emplaced plutons (Figure 9).

Thermally induced decreases in effective pressure may aid in the generation of earthquakes of large magnitude, even if fluid potential energy release is negligible. The intrusion of a large pluton or an increasing regional heat flux will decrease the effective pressure over a large volume of rock. In regions of active tectonic stress the resultant effective pressure may exceed the rock strength and result in the release of large quantities of tectonically induced elastic strain energy.

Conclusions

We have shown that thermally induced decreases in effective pressure may be an important process in geologic environments characterized by increasing temperature, since moderate increases in temperature produce large increases in pore fluid pressure. This process is probably most active in hot pluton environments where it plays an important role in the intrusion process, the generation of cracks, fluid convection, and the generation of measurable seismic activity.

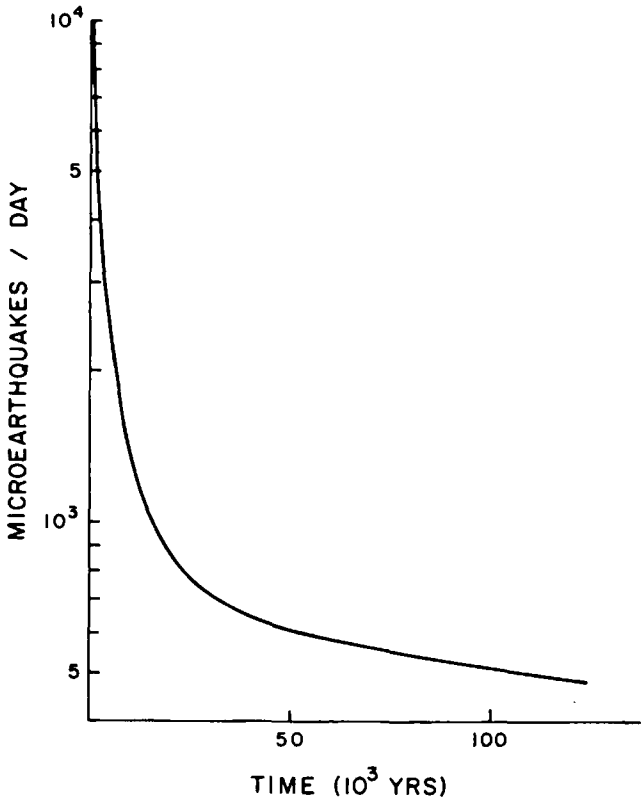

Fig. 9. Frequency of microearthquake production as a function of time after emplacement of the pluton. All events are magnitude zero.

Notation

$\underline{A}$	area normal to applied pressure, cm^2.
$\underline{D}$	elasticity matrix, dyn/cm^2.
E	energy, J.
$\underline{F}$	force, dyn.
$\underline{K}$	stiffness matrix, dyn/cm.
L_{ij}	length of element side with nodes i and j, cm.
l_{ij}	direction cosine of element side with nodes i and j.
M	earthquake magnitude (Richter surface waves).
m_{ij}	direction sine of element side with nodes i and j.
P	pressure, bar.
P_c	confining pressure, bar.
P_e	effective pressure, bar.
P_f	fluid pressure, bar.
P_I	initial pressure, bar.
P_o	equilibrium pressure, bar.
t	element thickness, cm.
T	temperature, °C.
$\underline{T}_{e,p}$	matrix that transforms nodal displacements into elemental strains, cm^{-1}.

$\underline{T}_{f,p}$ matrix that transforms the change in volume of a fluid element into nodal forces, dyn/cm^2.
$\underline{T}_{u,p}$ element interpolation matrix.
V volume, cm^3.
V_I initial volume, cm^3.
V_o equilibrium volume, cm^3.
α coefficient of volumetric-isobaric thermal expansion, $^oC^{-1}$.
β coefficient of isothermal compressibility, bar^{-1}.

Acknowledgments. This study was undertaken as a result of a discussion with D. L. Norton. His enlightened guidance and helpful suggestions are deeply and sincerely appreciated. We thank H. Kamel for his valuable contribution in the development of the constant mass fluid element and for the basic computer program. We are grateful to H. C. Helgeson and David Kirkham for providing programs to compute the state properties in the H_2O system. We also thank L. McLean for many improvements to the manuscript. All computing was done at the University of Arizona Computer Center. This study was supported by NSF grant EAR74-03515 A01.

References

Barker, C., Aquathermal pressuring--Role of temperature in development of abnormal-pressure zones, Amer. Ass. Petrol. Geol. Bull., 56, 2068-2071, 1972.

Bath, M., Earthquake energy and magnitude, Phys. Chem. Earth, 7, 117-165, 1966.

Belytschko, T., and J. M. Kennedy, Finite element study of pressure wave attenuation by reactor fuel subassemblies, J. Pressure Vessel Technol., 97, 172-177, 1975.

Birch, F., Compressibility, elastic constants, Handbook of Physical Constants, edited by S. P. Clark, Geol. Soc. Amer. Mem. 97, 97-174, 1966.

Combs, J., Heat flow and microearthquake studies, Coso geothermal area, China Lake, California, final report, ARPA order 1800, 65 pp., Advan. Res. Proj. Agency, Dallas, 1975.

Helgeson, H. C., and D. H. Kirkham, Theoretical prediction of the thermodynamic behavior of aqueous electrolytes at high pressures and temperatures, I, Amer. J. Sci., 274, 1098-1198, 1974.

Hubbert, M. K., and W. W. Rubey, Role of fluid pressure in mechanics of overthrust faulting, I, Geol. Soc. Amer. Bull., 70, 115-166, 1959.

Hubbert, M. K., and D. G. Willis, Mechanics of hydraulic fracturing, Trans. Soc. Petrol. Eng. AIME, 210, 153-166, 1957.

Jaeger, J. C., Cooling and solidification of igneous rocks, in Basalts, vol. II, edited by H. Hess, pp. 504-535, John Wiley, New York, 1968.

Jarzabek, D., and J. Combs, Microearthquake survey of the Dunes KGRA, Imperial Valley, Southern California (abstract), Geol. Soc. Amer. Abstr. Programs, 8, 939, 1976.

Johnson, D. M., and J. Combs, Microearthquake survey of the Kilbourne Hole KGRA, South Central New Mexico (abstract), Geol. Soc. Amer. Abstr. Programs, 8, 942, 1976.

Keenan, J. H., F. G. Keyes, P. G. Hill, and J. G. Moore, Steam Tables, 162 pp., John Wiley, New York, 1969.

Keller, G. V., Electrical studies of the crust and upper mantle, in The Structure and Physical Properties of the Earth's Crust, Geophys. Monogr. Ser., vol. 14, edited by J. C. Heacock, pp. 107-126, AGU, Washington, D. C., 1971.

Landisman, M., S. Mueller, and B. J. Mitchell, Review of evidence for velocity inversions in the continental crust, in The Structure and Physical Properties of the Earth's Crust, Geophys. Monogr. Ser., vol. 14, edited by J. C. Heacock, pp. 11-34, AGU, Washington, D. C., 1971.

Lovering, T. S., Theory of heat conduction applied to geological problems, Geol. Soc. Amer. Bull., 46, 69-84, 1935.

Minakami, T., S. Utibori, M. Yamaguchi, N. Gyoda, T. Utsunomiya, M. Hagiwara, and K. Hirai, The Ebino earthquake swarm and the seismic activity in the Kirisima volcanoes in 1968-1969, 1, Hypocentral distribution of the 1968 Ebino earthquakes inside the Kakuto Caldera, Bull. Earthquake Res. Inst., 47, 721-743, 1969.

Norris, R. J., and R. W. Henley, Dewatering of a metamorphic pile, Geology, 4, 333-336, 1976.

Norton, D., and R. Knapp, Transport phenomena in hydrothermal systems: The nature of porosity, Amer. J. Sci., in press, 1977.

Norton, D., and J. Knight, Transport phenomena in hydrothermal systems: Cooling plutons, Amer. J. Sci., in press, 1977.

Nur, A., and G. Simmons, The origin of small cracks in igneous rocks, Int. J. Rock Mech. Mining Sci., 7, 307-314, 1970.

Quillin, R., and J. Combs, Microearthquake survey of the Radium Springs KGRA, South Central New Mexico (abstract), Geol. Soc. Amer. Abstr. Programs, 8, 1055, 1976.

Skinner, B. J., Thermal expansion, in Handbook of Physical Constants, edited by S. P. Clark, Geol. Soc. Amer. Mem. 97, 75-96, 1966.

Walsh, J. B., The effects of cracks on the compressibility of rock, J. Geophys. Res., 70, 381-389, 1965.

Zienkiewicz, O. C., The Finite Element Method in Engineering Science, 521 pp., McGraw-Hill, New York, 1971.

(Received October 8, 1976;
revised December 22, 1976;
accepted January 5, 1977).